We are IntechOpen, the world's leading publisher of Open Access books Built by scientists, for scientists

6,900
Open access books available

186,000
International authors and editors

200M
Downloads

154
Countries delivered to

Our authors are among the

TOP 1%
most cited scientists

12.2%
Contributors from top 500 universities

CLARIVATE ANALYTICS
BOOK CITATION INDEX
INDEXED

WEB OF SCIENCE™

Selection of our books indexed in the Book Citation Index
in Web of Science™ Core Collection (BKCI)

Interested in publishing with us?
Contact book.department@intechopen.com

Magneto-Elastic Resonance: Principles, Modeling and Applications

Yannick Le Bras and Jean-Marc Greneche

Additional information is available at the end of the chapter

Abstract

The magnetostriction effects are first discussed in the frame of the magneto-elastic resonance to define important values mainly the magneto-elastic coupling factor, k_{33}. We review the different magnetostrictive materials according to their developments, with a special attention to amorphous ribbons to design magnetostrictive resonators. Furthermore, we focus on the current instrumental setups including their limitations, and then on the usual measurement procedures of the resonators, particularly the frequency domain measurement. In addition, an innovative approach based on the magneto-elastic impedance is reported, together with an analytical model which establishes the complete transfer function between the input and output voltages. This model is applied to ribbon-shaped materials, particularly to determine the magneto-elastic coupling factor. These resonators are suitable to sensing applications, i.e., to estimate the influential quantities such as the temperature, magnetic fields and mass stuck on the resonating surface.

Keywords: resonant frequency, magnetostrictive resonators, magneto-mechanical coefficient, analytical model, sensor

1. Introduction

This chapter deals with the magneto-elastic resonance: this form of mechanical resonance involves magneto-mechanical properties of some ferromagnetic materials. Consequently, it presents some similarities to other types of resonance, such as the existence of resonant and anti-resonant frequencies. The behaviors of magnetostrictive resonators, which also result from magneto-mechanical properties, give rise to some specific particularities. After introducing the main features on magneto-elastic resonance, we first report on the magnetostriction effects and the relevant characteristics of subsequent materials in order to design magnetostrictive resonators. Then, we detail an analytical model in the case of a ribbon-shaped

resonator allowing the magneto-elastic coupling factor to be estimated. Finally, we propose some resonator based on a magnetostrictive amorphous ribbon, which behaves as a good platform for sensing applications while we report on the emblematic example of freezing-rain sensor.

2. Magnetostriction effects

Resonance could be defined as a phenomenon that occurs when a vibrating system has greater amplitude at some specific resonant frequencies. In case of magneto-elastic resonance, the vibrating system can be established from a magnetostrictive material. One can consider, in a first approach, this mechanical resonance occurs with a magnetic cause. To obtain the excitation, i.e., a mechanical vibrating strain, one applies a vibrating magnetic field and the magnetostriction converts magnetic variation into strain variation. In return, when resonance occurs, strain is at a maximum. As a consequence of magnetostrictive effects, magnetic values are also at maxima resulting from maximum of mechanical values. Thus, magneto-elastic resonances result from mechanical and magnetic resonances. Consequently, studying magneto-elastic resonance requires knowing of magnetostriction effect, as presented in the next section.

2.1. Magnetostriction

2.1.1. Definition

Magnetostriction can be defined, in a first approach, as the property of some ferromagnetic materials to modify their shape due to change in magnetization [1, 2]. In practice, only some ferromagnetic materials have significant shape and magnetization correlated changes. This phenomenon was discovered by James Prescott Joule in 1842 studying a sample of iron. Since Joule's discovery, many magnetostriction effects have been highlighted, such as bending, torsion, density changes, or Young's modulus variations. We still use the term of magnetostriction for all magneto-elastic properties. This chapter is only concerned by changes in shape. More precisely, two effects are involved in common magnetostrictive resonators, the Joule and Villari effects; the last one corresponds to the inverse magneto-elastic effect.

2.1.2. Joule and Villari effect

A ferromagnetic material with parallelepiped shape elongates or shrinks under a magnetic field according to the longitudinal Joule effect. The reversal effect, change of magnetization while submitted to a mechanical stress is known as Villari effect. These effects are depicted by the material magnetostriction curves which describe the variation of the relative deformation $\lambda = \frac{dL}{L}$, where L is the length of the sample, versus H the magnetic field applied to the material.

A typical curve is characterized by a maximum, as illustrated in **Figure 1**; in addition, one clearly observes some hysteresis also commonly called "butterfly loop," because of its symmetrical shape. In the next part, curves are restricted to the positive fields. The asymptotic
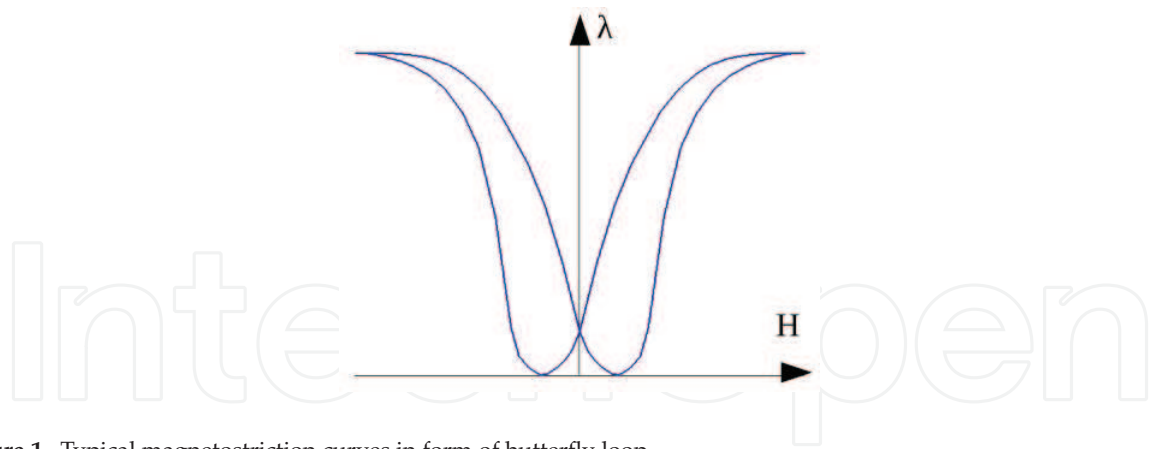
Figure 1. Typical magnetostriction curves in form of butterfly loop.

elongation or shrinkage gives rise to magnetostriction at saturation: the maximum value λ_s corresponds to the saturation magnetostrictive coefficient, i.e., the strength of the magneto-elastic coupling, which can be thus either positive or negative, respectively. It is usually found in the order of 10^{-6} but could rise up to 10^{-3} in the case of Terfenol-D ($Tb_xDy_{1-x}Fe_2$, x ~ 0.3), which behaves as the best magnetostrictive material and is commonly applied as engineering magnetostrictive material. The magnetostriction can be described by a quadratic function and the sign is strictly dependent on the material, not on the direction of the applied magnetic field. Note that it differs from piezomagnetism (analogously piezoelectric effect), which is character-ized by a linear coupling between the mechanical strain and the magnetic polarization.

It is important to emphasize that function $\lambda(H)$ is not linear and could be more rugged than the typical one illustrated in **Figure 1**. Indeed, $\lambda(H)$ is not strictly monotonous (as for Fe), for which one can distinguish two regimes with positive and negative values of λ, corresponding to an elongation and shrinkage of material for small and larger fields, respectively.

In addition, the deformation is not exclusively dependent on the magnetic field. Indeed, among the other parameters, the temperature plays an important role: when the temperature increases, the elongation decreases as the magnetization is reduced. The magnetostriction curves also depend on the direction of the applied field respect to the easy magnetization axes, i.e., the shape and the chemical purity of the sample and also on its thermomagnetic history.

2.1.3. Causes

The physical mechanisms of the magnetostrictive effects have not been yet described successfully at the atomic scale, to the best of our knowledge. But they are not necessary for our current topic. On the opposite, we would only keep in mind a simple picture, as schematized in **Figure 2**: the main idea is based on the rotation of magnetization in presence of an external magnetic field, which may originate some new arrangements of magnetic domains causing either elongation or shrinkage of the magnetostrictive material [3].

One can distinguish different contributions to the magnetic energy from nano to microscale: exchange interactions, dipolar interactions, magneto-crystalline anisotropy, shape, interface,
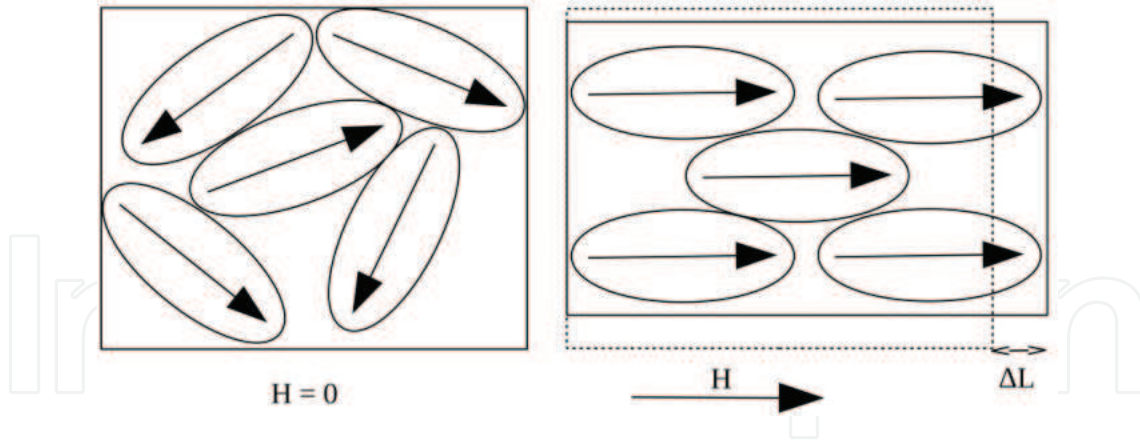
Figure 2. Schematic picture depicting the magnetostriction caused by rotation of magnetization.

and magneto-elastic anisotropy energies. When the material is submitted to mechanical stresses and/or an external magnetic field, the equilibrium of the deformations corresponds to the minimum of the total energy. In the case of a crystalline magnet, the application of uniaxial mechanical stress originates a magnetostrictive contribution to the magnetic anisotropy. It is clear that this magneto-elastic contribution results from the magneto-crystalline term: indeed, under stress crystals can be considered as stressless crystals with a slightly different crystalline structure. In the case of polycrystalline materials, the saturation magnetostriction is an average over different crystal orientations.

Magnetostrictive materials are suitable to convert magnetic into kinetic energy and vice-versa: they can be thus applied to design actuators and sensors. They are implemented in sonars, generation of ultrasound for medical, industrial uses, or for active control of noise and vibration, using simultaneously the opposite effect for vibration measurement and the direct one to carry out the corrective action.

2.2. Characteristic quantities, magneto-elastic coupling factor

2.2.1. Curves, magnetostriction at saturation and slope

The useful information expected by engineers and technicians is the magnetostriction curve, as plotted in **Figure 1**, which characterizes the magnetostrictive material [4]. Indeed, one could easily define the maximum of deformation and estimate λ_s which is usually reported by the manufacturer in the literature. This value presents the advantage to be unequivocal and weakly dependent on further physical parameters except temperature.

This value is able to predict the maximum change in length as $\Delta L_{max} = \lambda_s \cdot L$ but does not describe the sensitivity of the magneto-mechanical conversion. But the slope $d = \left(\frac{\partial \lambda}{\partial H}\right)_\sigma$ is a useful representation of materials properties, since it indicates how rapidly the strain changes with the relevant applied field, according to Jiles [5]. The largest slope, d_{max}, corresponds to the best operating point. But, it is important to emphasize that literature does not report on d_{max}

but on λ_s, because of some dependencies on influence quantities (especially d_{max}, sometimes noted d_{33}, depends on the direction of the magnetic field).

2.2.2. Magneto-mechanical coupling coefficient k_{33}

The more relevant characteristic of a resonator is obviously the magneto-mechanical coupling coefficient k_{33}, a dimensionless parameter, which describes the energy conversion as $k_{33}{}^2$ is the energy conversion ability from magnetic into elastic energy and inversely. The values of k_{33} which can be estimated from the slope of the curve are expected to be theoretically ranged from 0 up to 1. The larger value which is 0.97 has been observed for an amorphous metallic ribbon.

Du Trémolet de Lacheisserie has proposed an equation to estimate the effective magneto-mechanical coupling k_{33} coefficient from the calculation of Gibbs free energy, as

$$k_{33} = d_{33}\sqrt{\frac{Y^H}{\mu_{33}{}^\sigma}} \tag{1}$$

where, $\mu_{33}{}^\sigma$ is the permeability at constant stress and Y^H the Young's modulus at constant field (certain conditions are reported in a next section). Indeed, the effective value of k_{33} depends on the boundary conditions (geometry and fixation of the magnetostrictive material acting as resonator) and the mode of induction of the magnetic field.

2.3. Materials

Since Joule and his discovery of magnetostriction on an iron sample, many new magnetostrictive materials have been identified [3, 5, 6]. Hartemann proposed [1] to classify them into four main categories: nickel and metallic crystalline alloys, the first materials to be used, ferrites, iron-rare-earth alloys, and amorphous alloys. But, this classification has to be updated with nanocrystalline alloys as obtained from subsequent annealing on as-quenched alloys on one hand, and the newer Fe-Ga based alloy (Galfenol) on the other hand.

2.3.1. Nickel, metallic alloys, and magnetostrictive ferrites

Polycrystalline nickel was the first magnetostrictive material to be used as a transductor. **Figure 3** compares the magnetostriction curves characteristics of Ni (thick) and Fe (thin), revealing negative and positive magnetostriction coefficient, respectively.

Nickel which is semi-soft (or semi-hard) magnetic material, gives clear evidence for a quite large linearity range with a magnetostriction at saturation λ_s of -35 ppm and a magneto-mechanical coefficient k_{33} of 0.3. In addition to a significant hysteresis, Ni characteristics are strongly dependent on its chemical purity and the annealing conditions to get polycrystalline structure: nevertheless Ni remains an excellent standard. As abovementioned, λ_s (Fe) depends on the external field, giving rise to positive and then negative magnetostrictive behavior.
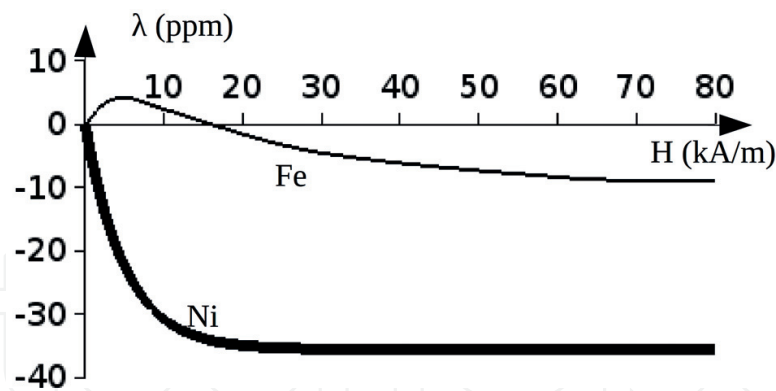
Figure 3. Magnetostriction curves characteristic of Ni (thick) and Fe (thin).

The magnetostrictive properties of Fe-Ni alloys result from a combination of their respective positive and negative magnetostrictive and magneto-crystalline anisotropies: it allows different magnetostrictive characteristics to be tuned as a function of the chemical content. Thus, Permalloy has high permeability and magnetostriction near zero for Permalloy 78 (78% Ni) but Permalloy 45 is greatly magnetostrictive ($\lambda_s = 27 \times 10^{-6}$, $k_{33} = 0.3$). **Table 1** lists some physical characteristics of iron-aluminum (Alfenol), nickel-cobalt, and iron-cobalt alloys.

In the case of ferrites with spinel structure, the magnetic properties are not only dependent on the nature of cations, but also on their distributions into the tetrahedral and octahedral sites giving rise to either direct, inverse, or mixed structures. Consequently, the conditions of elaboration using the ceramic route, the chemical nature, and content of their atomic elements provide large varieties of materials. Co-based ferrites are excellent candidates as magnetostrictive materials (see characteristics listed in **Table 1**, in addition to their high resistivity compared to those of

Material	λ_s (ppm)	k_{33} max ()	d_{33} max [6] $_{(10^{-9}\ m/A)}$
Fe	−9		0.3
Ni	−35	0.3	−3
Co	−62		−0.2
Permalloy 45 (Ni45-Fe55)	27	0.3	
Permalloy 80 (Ni80-Fe15-Mo5)	<1.2		
Alfer 13 (Al 13-Fe 87)	40	0.3	
Co 4.5-Ni 95.5	−36	0.5	
Fe 30-Co 70 laminated	130		
Ferrites Fe_3O_4	40	0.36	
Ferrites $CoFe_2O_4$	−110		
Terfenol ($TbFe_2$)	1753	0.35	
Terfenol-D ($Tb_{0.3}Dy_{0.7}Fe_2$)	1100	0.75	57
Galfenol	250	0.7	

Table 1. Specific characteristics (λ_s, k_{33max}, d_{33max}) of some selected magnetostrictive materials.

metal alloys). Microferrites can then be used at higher frequencies, but their mechanical fragility remains a serious weakness.

Nickel and metal alloys are used mainly as actuators for applications requiring small displacements with a large force like for ultrasound emission.

2.3.2. Iron-rare-earth compounds

As noted by du Trémolet de Lacheisserie, studies developed on iron-rare-earth compounds are exemplary in the field of magnetic materials. The aim of the researchers was to combine advantages of 3d metals and/or alloys able of operating at room temperature and under relatively small magnetic fields, but with poor magnetostrictive effects and 4f metals which exhibit high values of magnetostriction coefficient but very low Curie temperatures. Those studies developed in the 70's led to significantly improved magnetostrictive materials with deformations 50–100 times larger. Thus, Clark first developed the $TbFe_2$ alloy named Terfenol (TERbium, FEr, Naval Ordnance Laboratory), which exhibits a relatively high Curie temperature with giant magnetostriction but with a great magneto-crystalline anisotropy. Then, he elaborated a mixed alloy combining two different rare-earth species, giving rise to $Tb_{0.3}Dy_{0.7}Fe_2$ which exhibits rather similar advantages than Terfenol but is easier to be magnetically saturated ($\lambda_s = 1100 \times 10^{-6}$, $k_{33} = 0.75$). Terfenol compounds which behave as hard magnets are brittle and expensive. According to its characteristics, Terfenol-D remains currently an excellent magnetostrictive material. Indeed, it is suitable to be applied as magnetostrictive actuator at room temperature, but with restriction in use as resonator. We report magnetostriction curve under preload (**Figure 4**): it appears different curves and in particular, the maximum slope of the curves reported are 15, 80, and 40 10^{-9} A/m for pressures of 0, 20, and 40 MPa, respectively. Such values are greater than those predicted by du Trémolet de Lacheisserie [4].

It is important to emphasize that, as observed in its website [7], Etrema™ reports the curve established without load which does not allow correct values of k_{33} to be extrapolated; indeed, as illustrated in **Figure 4**, the values of the magneto-mechanical coefficient can be well estimated providing that the material (Terfenol-D) is submitted to important loads. Thus, one has
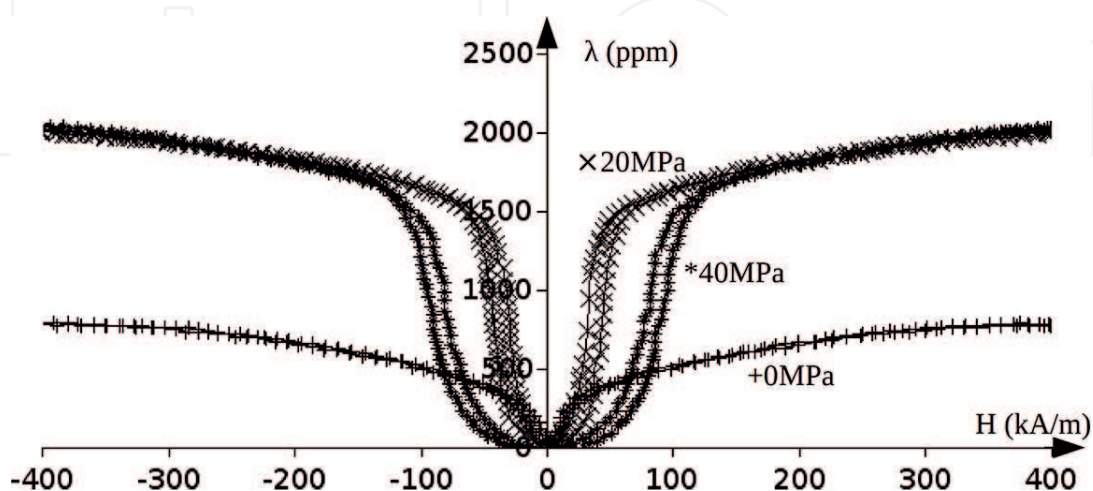

Figure 4. Magnetostriction curve characteristic of Terfenol-D with and without preloading.

to be very careful to estimate the value of k_{33}. In addition, most of resonators work without load, making that Terfenol cannot act as an excellent magnetostrictive material, contrarily to Ni which possesses a large k_{33} value with a small polarization.

2.3.3. Amorphous and nanocrystalline material

In the case of usual resonators, the highest values of magnetostriction coefficient are not strictly necessary but the key parameter does result from the largest possible magnetostrictive effect obtained in presence of a magnetic field as small as possible, i.e., large d and k_{33} values [6, 8]. Some ribbon-shaped amorphous glasses possess very good magneto-elastic properties (great k_{33} for small field) associated to excellent mechanical properties. Let us remember that the metallic amorphous ribbons, also called metallic glasses, are obtained by rapid quenching from the induction melt (10^6 K/s) using the roller technique: a molten alloy is ejected by a flume onto a cooled rotating wheel. The experimental conditions (temperature of the melt, size of capillary, distance capillary-wheel, nature and surface state of the wheel, protective gas, etc.) have to be optimized to get regular ribbons over large lengths (up to several km). Their thicknesses—typically ranged from 20 to 40 μm—favor some mechanical brittleness which depends on quenching conditions. The amorphous ribbons are usually soft magnets with relative permeability more than 10^5 and coercive field near 1 A/m, very low magneto-crystalline anisotropy while their magnetostrictive properties are strongly correlated to their chemical composition (particularly that of Fe, Ni, and Co). The magnetic properties can be improved by annealed under a magnetic field, transverse to increase magnetostriction (longitudinal to annihilate). The largest magneto-mechanical coupling coefficient k_{33} was measured on Metglas 2605SC ribbon annealed at 390°C under a transverse in-plane magnetic field of 400 kA/m for approximately 10 min. The magneto-mechanical coupling coefficient k_{33} is close to 1. We report technical properties of two ribbons of metallic glasses, the best 2605SC and the most used 2826 MB.

As listed in **Table 2**, the main characteristics of metallic amorphous ribbons make them good candidates as magnetostrictive resonators (soft magnet, mechanically soft, large k_{33}), despite their weak thicknesses. Nanocrystalline alloys (such as FINEMET, NANOPERM, and HITP ERM) which result from a subsequent annealing of the amorphous precursor do not exhibit better magnetostrictive characteristics. An alternative is related to bulk amorphous glasses (BMG) which could be obtained as cylindrical rods by mold casting and suction casting techniques: some of them possess excellent soft or hard magnetic properties with saturation magnetostriction values ranged up to 40×10^{-6}.

3. Magnetostrictive resonator

3.1. Structure

Resonators consist of a magnetostrictive material, one or two exciting coils, one or two pick-up coils and eventually a support (a schematic view is given in **Figure 5**) [9, 10]. Exciting coil, either Helmholtz type or a rather long cylindrical coil, aims to produce a homogeneous magnetic field with an alternating component and a DC component. Exciting coil converts vibrating current into vibrating field. This field induces vibrations in the ribbon-shaped material with a resonant frequency which is dependent on its size, usually length L.

Properties	Units	Metglas 2605SC	Metglas 2826 MB
Composition		$Fe_{81}B_{13.5}Si_{3.5}C_2$	$Fe_{40}Ni_{38}B_4Mo_{18}$
Thickness	(μm)	17	29.2
Density	kg.m^{-3}	7320	7900
Magnetostriction at saturation	(ppm)	30	12
Magneto-mechanical coupling coefficient	—	0.97 (H = 50 A/m)	0.3
Crystallization temperature	K	480	410
Young's modulus	GPa	25	100-110
Résistivité électrique	μ.Ω.m	1.35	1.38
Perméabilité relative maximum	—	300,000	800,000

Table 2. Specific physical parameters characteristic of two ribbon-shaped metallic glasses.
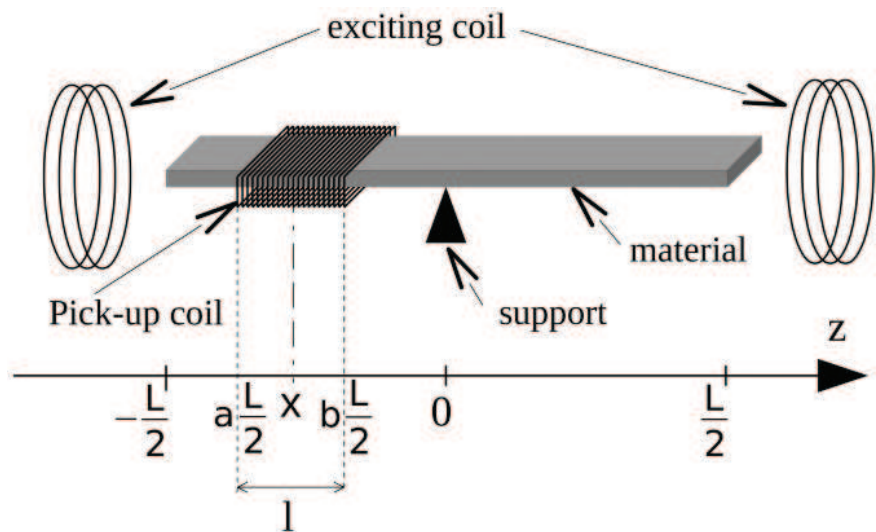

Figure 5. Principle of a ribbon-shaped resonator.

As described by Grimes [10], vibrations "can be detected magnetically with a pick-up coil, acoustically with a microphone, or optically with a laser emitter and a photo-transistor." Next, we focus on resonators with vibration detection based on the Villari effect, resulting from the pick-up coil as previously mentioned.

Ideally, the best configuration would be to study a free ribbon, thus in practice, the ribbon does simply lye on a flat and smooth surface or be centered in its middle on a support.

3.2. Operating principle, elementary model

A generator delivers a current with an alternating component to the excitating coil which in turn generates a magnetic field proportional to the current. The magnetostrictive material subjected to the field, is thus deformed. By applying a sinusoidal current component, the material vibrates according to a sinusoidal mode. The excitation is the strains originated from field's variation, and the resonator acts thus as a mechanical resonator.

The resonator with parallelepiped shape could be modeled as a plate, where ultrasound waves propagate without losses. Assuming a one-dimensional problem and choosing as system a slice of thickness dx, its mass is

$$dm = \rho \cdot h \cdot e dx \tag{2}$$

where h, e, and ρ are the thickness, depth, and the density of the plate, respectively.

The balance of forces represented in **Figure 6** provides $\overrightarrow{f(x)} = \sigma(x) \cdot S \cdot \overrightarrow{x}$ and $\overrightarrow{f(x+dx)} = -\sigma(x+dx) \cdot S \cdot \overrightarrow{x}$, where S is the cross-section of the resonator.

When applying fundamental principle of dynamics, it comes out:

$-\sigma(x+dx)S + \sigma(x)S = \rho S dx \frac{\partial^2 u}{\partial t^2} \Rightarrow -\frac{\partial \sigma}{\partial t} = \rho \frac{\partial^2 u}{\partial t^2}$, where u is the displacement.

From both the Hooke's law establishing the proportionality between relative elongation and constraint, $\lambda = \frac{-1}{Y} \cdot \sigma$, and the expression of the elongation is given as

$$\lambda = \frac{dL}{L} = \frac{u(x+dx) - u(x)}{dx} = \frac{\partial u}{\partial x} \tag{3}$$

one gets $\frac{\partial^2 u}{\partial t^2} - \frac{1}{c^2} \frac{\partial^2 u}{\partial x^2} = 0$ where $c = \sqrt{\frac{Y}{\rho}}$.

This equation can be solved using harmonic solutions $u(t,x) = e^{j2\pi ft} \cdot u(x)$ with

$u(t,x) = U_1 e^{j\frac{2\pi f}{c}x} + U_2 e^{-j\frac{2\pi f}{c}x}$ and assuming constraint at x = 0 with u(0)=0 and boundary conditions $\sigma\left(\frac{L}{2}\right) = \sigma\left(-\frac{L}{2}\right) = 0$.

Consequently, $\sigma(x) = -j2Y \frac{U \cdot 2\pi f}{c} \cos\left(\frac{2\pi f}{c}x\right)$, to satisfy $\sigma\left(x = \frac{L}{2}\right) = 0$ involving $\frac{2\pi f}{c}L = \pi(2p+1)$ where p is a positive integer.

Resonances are established at frequencies $f_p = (2p+1)\frac{c}{2L} = \frac{(2p+1)}{2L} \cdot \sqrt{\frac{Y}{\rho}}$, and particularly the fundamental frequency corresponding to that characteristic of the material:

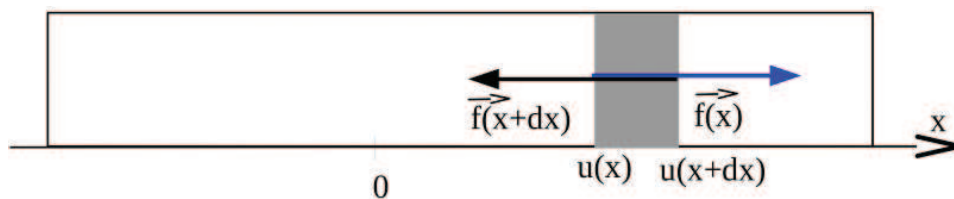$$f_0 = \frac{1}{2L} \cdot \sqrt{\frac{Y}{\rho}}. \tag{4}$$

Figure 6. Resonator modeling, with the stress forces.

3.3. Measurement

By Villari effect, resonator's vibration generates a time-varying magnetic flux, measured by the pick-up coils. Three different routes as time domain measurement, frequency domain measurement, and magneto-elastic impedance can convert this variation to estimate f_0.

3.3.1. Time domain measurement

The strategy consists in exciting the resonator to its natural frequency. Then, one could apply to the exciting coil a rectangular wave-train pulse, or even better, a sinusoidal wave-train, as the current variation is limited by the inductance. Then the response, the pick-up coil's voltage, is a damped sine wave-train (**Figure 7**). The natural frequency can be thus determined by fast Fourier transform (FFT), frequency counting or demodulation. FFT gives the spectrum of the voltage which maximum corresponds to the natural frequency. Furthermore, frequency counting consists in the determination of a number of oscillations. Thus, a comparator converts the voltage into a rectangular shape voltage whose frequency can be easily determined by a counter, according to the definition of a frequency. The last technique consists in demodulating the pick-up's signal: a phase-locked loop replaces the counter and gives voltage corresponding linearly to the frequency. The frequency counting and demodulation techniques require less high-performance instrumentation but remain more difficult to be well achieved. On the contrary, FFT gives *a priori* better results and particularly the quality factor characteristics of the resonance.

3.3.2. Frequency domain measurement

The resonant frequency results from the transfer function. The excitation coil is connected to a function generator and the pick-up coil to a voltage measurement system. The generator delivers a sinusoidal voltage as a function of frequency (sweeping mode) giving rise to V(f) corresponding to the amplitude of the pick-up coil (as illustrated in **Figure 9b**). The resonant frequency corresponds to the maximum. This measurement can be carried out using only a spectrum analyzer that delivers the magnitude of the input signal versus frequency: such an approach allows the resonant frequency, the anti-resonant frequency, and the resonance quality to be obtained.
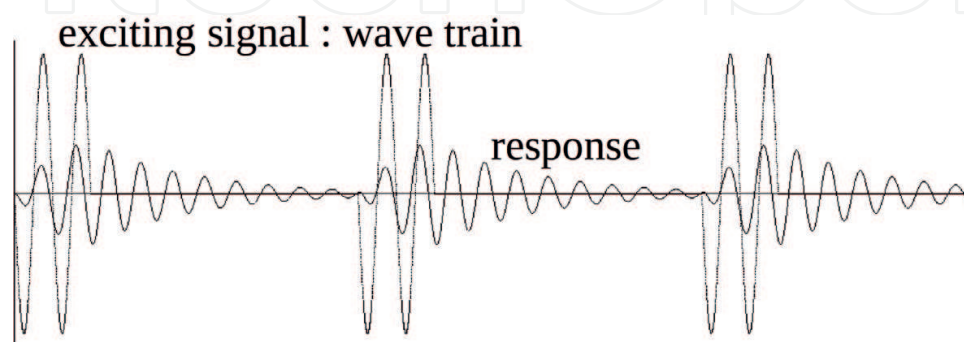

Figure 7. Time domain measurement signals: wave train and response as continous and dashed line, respectively.

3.3.3. Magneto-elastic impedance

The experimental setup for measuring the evolution of the impedance is close to that of frequency domain measurement. An analyzer measures real and imaginary parts of voltage as a function of the frequency, allowing thus the variation of impedance which is experimentally similar to the transfer function versus frequency. Let us note that the instrumentation is similar for the two techniques, but physicists prefer the later one which also gives the evolution of the permeability.

3.4. Development

The development of a resonator requires a setup comprising polarization and excitation coils (possibly one for both), two pick-up coils, a continuous power supply, and an analyzer, in addition to the magnetostrictive material. Consequently, its achievement is not a difficult task providing some rules to be satisfied.

3.4.1. The resonator

As concluded in Section 2.2, the main criterion of choice is the magneto-mechanical coefficient or the slope of curves $\lambda(H)$, i.e., a material with a k_{33} at least more than 10%, for a DC field easy to obtained in the lab. For preliminary tests, Ni foil or amorphous 2826MB would be a good choice according to Section 2.3, but the optimal choice depends on the application.

The output is often the resonant frequency that is inversely proportional to the length of the resonator with parallelepiped shape. To get an acute resonance, the resonator requires a strictly constant length L: consequently, the cutting has to be done with extreme caution. Different techniques such as paper guillotine, laser beam, diamond wire saw, or electrical discharge machining have to be optimized according to the brittleness of the material and preventing from contamination and from crystallization in the case of amorphous ribbons. After cutting, the material may undergo subsequent treatment under field in neutral atmosphere to improve magnetostriction.

3.4.2. Coils and electrical setup

Polarization and excitations coils such as Helmholtz or long cylindrical solenoid, do create a uniform field. In addition, as the field produced by a coil is proportional to the current, it is easier to get only one coil, using links capacitor and inductor to discriminate the DC and AC component voltage (see **Figure 8**). The advantage of Helmholtz coils is that the resonator is placed outdoor, but as the field decreases with the square of the coil diameter, a large coil creates a greater field than Helmholtz type with the same current.

The coil picks up the time derivative of flux $\Phi_n = \mu_0 H \cdot S_n + \mu_0 M \cdot S_{rib}$ resulting from n loops of surface S mounted around the material. Then the flux is image of the magnetization M, but also of the magnetic field H. The field component is removed using a differential measurement from two pick-up coils. Indeed, the second coil is identical to the first one and placed, out of the material, symmetrically centered in the excitation field, what measured is the voltage of the
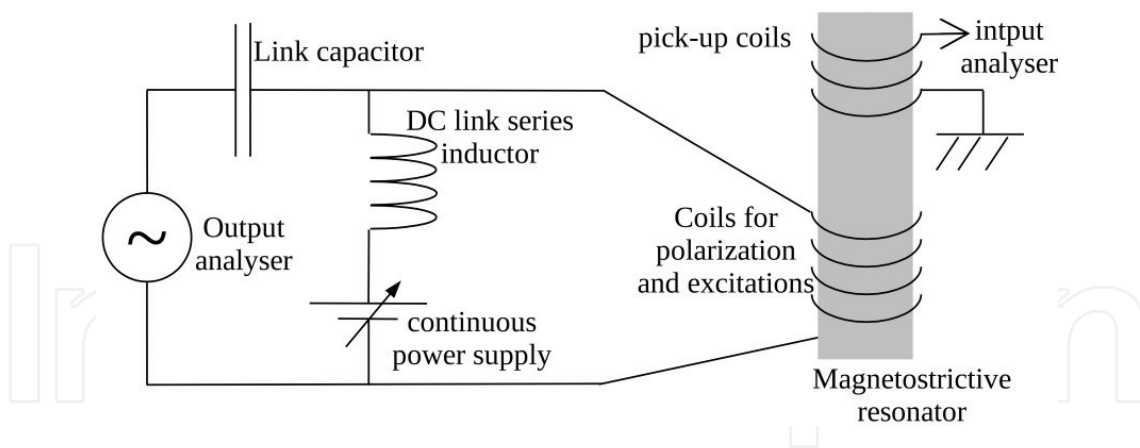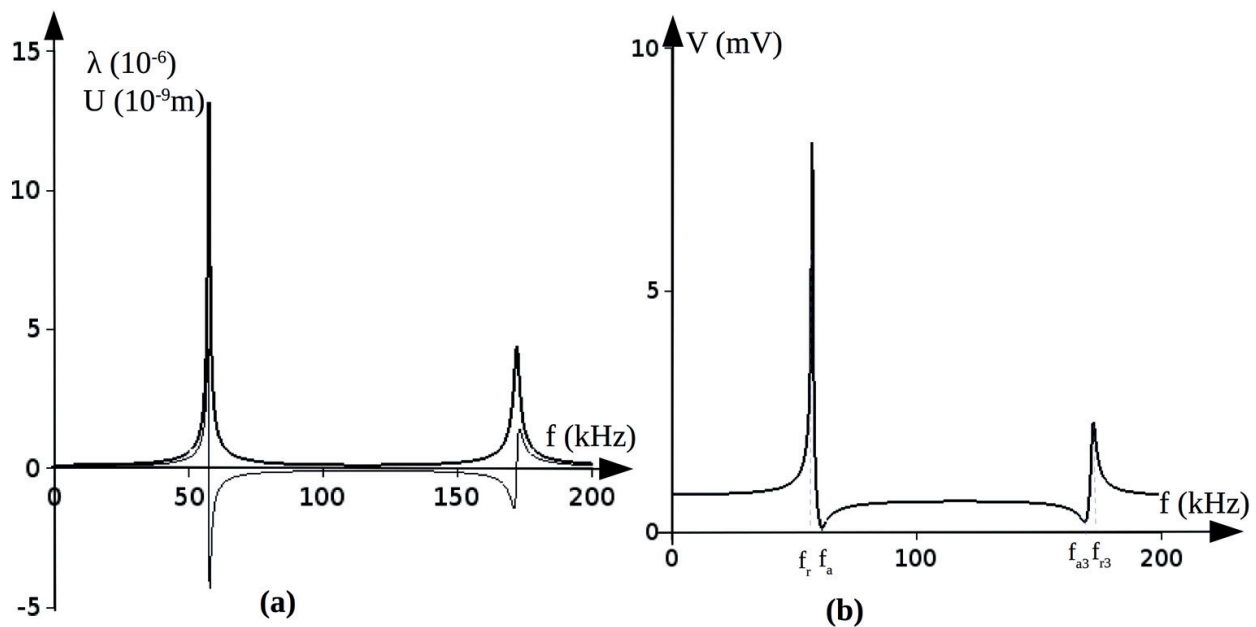
Figure 8. Coils and electrical setup.

Figure 9. a: Examples of frequencies responses of the maximum strains in the middle (thick,) and displacement at the ends (thin). b: Examples of frequencies responses of the pick-up coil's voltage.

serial coils: $u = n \frac{d(\mu_0 M \cdot S_{rib})}{dt}$. The voltage u is thus proportional to the derivative of the magnetization change with the sinusoidal strain.

3.4.3. Setting

The first step consists in determining the place of the pick-up coil corresponding to a minimum of voltage without resonator in order to optimize the compensation. Then, the measuring range has to be refined from an approximate value of the resonant frequency. The resonance is obtained by adjusting first the amplitude of the excitation at around 1 V and scanning the DC voltage. The final refinement of the position of the pick-up coil and the amplitude of the AC voltage gives rise to a curve similar to that displayed in **Figure 9b**.

4. Analytical model

An analytical model is thus necessary to estimate the frequency dependence of the output/input coils voltage ratio when submitted to an electrical excitation [11]. It consists in establishing the equations coupling mechanical and magnetic quantities.

4.1. Modeling and assumptions

3D general equations can be derived into the two following 1D Eqs. (5) and (6), assuming a low AC component of the magnetic field

$$\widetilde{B} = d \cdot \widetilde{\sigma} + \mu^{\sigma} \cdot \widetilde{H} \tag{5}$$

$$\widetilde{\lambda} = \frac{1}{Y} \cdot \widetilde{\sigma} + d \cdot \widetilde{H} \tag{6}$$

where $\widetilde{X}$ refers to a low level AC quantity, B, H, ε, σ, Y, d, and μ^{σ} are the magnetizing flux density, the magnetic field, the strain, the stress, the Young modulus, the slope of the magnetostriction curve, and the magnetic permeability at constant stress, respectively.

The ribbon is assumed to be set in the middle. The magnetic field is uniform and has two components: H_{DC} and alternating $\widetilde{H}$ with $H_{DC} \gg \widetilde{H}$. In addition, $\widetilde{H}$ is low enough to neglect the effects of hysteresis. The complex Young modulus is expressed as $\overline{Y} = Y(1 + j\eta)$, where the imaginary part takes into account mechanical and magnetic losses with η, the damping factor characteristic of the resonator.

The boundaries conditions are related to the two ends of the ribbon mechanically free, except strains due to magnetostriction:

$$\lambda \left(z = -\frac{L}{2} \right) = \widetilde{\varepsilon_0} = d \cdot \widetilde{H} \tag{7}$$

$$\lambda \left(z = \frac{L}{2} \right) = \widetilde{\varepsilon_0} = d \cdot \widetilde{H} \tag{8}$$

The vibrations resulting from the excitation field are described by the wave propagation equation derived from Newton's second law:

$$\frac{\partial \sigma}{\partial t} = \rho \, \frac{\partial^2 u}{\partial t^2} \tag{9}$$

where u is the longitudinal displacement and ρ the density.

From Eqs. (3), (9), and (6), assuming that $\frac{\partial \widetilde{u}}{\partial z} = 0$ (uniform field), one gets

$$\overline{Y} \frac{\partial^2 \widetilde{\lambda}}{\partial z^2} = \rho \, \frac{\partial^2 \widetilde{\lambda}}{\partial t^2} \tag{10}$$

4.2. The strain expression

Eq (10) can be solved by using harmonic oscillations expressed as

$$\widetilde{\lambda}(z,t) = e^{j\omega t} \cdot E \cdot e^{jKz} \tag{11}$$

From Eqs. (10) and (11) $K = \pm(k_r + jk_i)$ with $k_r = \frac{\sqrt{\frac{\rho}{Y}} \cdot \omega}{\sqrt[4]{1+\eta^2}} \cos\left(\frac{tg^{-1}(\eta)}{2}\right)$ with $k_i = \frac{-\sqrt{\frac{\rho}{Y}} \cdot \omega}{\sqrt[4]{1+\eta^2}} \sin\left(\frac{tg^{-1}(\eta)}{2}\right)$.

Considering above boundary conditions, one finally obtains from Eq. (12):

$$\lambda(z) = d \cdot \widetilde{H}\left(E_{r0} + jE_{i0}\right)\left(e^{(-k_i + jk_r)z} + e^{(k_i - jk_r)z}\right) \tag{12}$$

With

$$E_{r0} = \frac{e^{\frac{3k_i L}{2}} + 3e^{\frac{k_i L}{2}} + 3e^{-\frac{k_i L}{2}} + e^{-\frac{3k_i L}{2}} - 4e^{\frac{k_i L}{2}}\cos^2\left(\frac{k_r L}{2}\right) - 4e^{-\frac{k_i L}{2}}\cos^2\left(\frac{k_r L}{2}\right)}{e^{2k_i L} - 2 + e^{-2k_i L} + 16\cos^2\left(\frac{k_r L}{2}\right) - 16\cos^4\left(\frac{k_r L}{2}\right)} \cos\left(\frac{k_r L}{2}\right)$$

$$E_{i0} = \frac{e^{\frac{3k_i L}{2}} + e^{\frac{k_i L}{2}} - e^{-\frac{k_i L}{2}} - e^{-\frac{3k_i L}{2}} - 4e^{\frac{k_i L}{2}}\cos^2\left(\frac{k_r L}{2}\right) + 4e^{-\frac{k_i L}{2}}\cos^2\left(\frac{k_r L}{2}\right)}{e^{2k_i L} - 2 + e^{-2k_i L} + 16\sin^2\left(\frac{k_r L}{2}\right)\cos^2\left(\frac{k_r L}{2}\right)} \sin\left(\frac{k_r L}{2}\right).$$

At this stage, the frequency variation of the strain can be plotted but the displacement at ends of the resonating ribbon is preferred. This second curve can be obtained by means of a contactless measurement as laser vibrometer or microphone.

The expression of the motion is determined from Eqs. (3) and (12):

$$u(z) = d \cdot \widetilde{H}\left(E_{r0} + jE_{i0}\right)\left(\frac{e^{(-k_i + jk_r)z}}{(-k_i + jk_r)} + \frac{e^{(k_i - jk_r)z}}{(k_i - jk_r)}\right)$$

Figure 10a reports the frequencies' responses of the maximum strain (in the middle) and displacement (at the ends) for a ribbon taken from an anti-theft which is Vitrovac 4040 ($Fe_{39}Ni_{39}Mo_4Si_6B_{12}$; ρ = 7400 kg.m^{-3} and L = 37 mm. The refined characteristics are k_{33} = 0.312, d = 20 × 10^{-9} m/A, H_{ACmax} = 4 A/m and η = 0.012.

The mechanical responses are quite different from the measurement based on the inverse magnetostrictive (Villari) effect (**Figure 9b**).

4.3. Expression of the frequency response

As coils associated with the magnetostriction convert mechanical quantities into electrical quantities, the next step consists thus in substituting mechanical by magnetic quantities.

From Eqs. (12), (5), and (1):

$$\mu = \frac{\widetilde{B}}{\widetilde{H}} = \mu^\sigma\left(1 - k_{33}^2 + k_{33}^2\left(E_{r0} + jE_{i0}\right)\left(e^{(-k_i + jk_r)z} + e^{(k_i - jk_r)z}\right)\right) \tag{13}$$
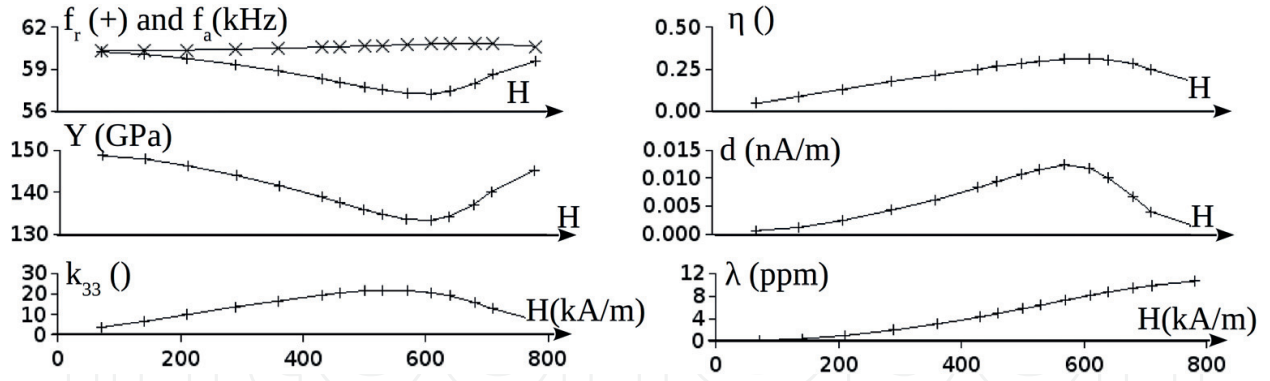
Figure 10. Evolution of resonant and anti-resonant frequency f_r (+) and f_a (x), Young's modulus Y, magneto-mechanical coefficient k_{33}, damping η, slope of the magnetostriction curves d, and strain λ as function of DC field for Vitrovac ribbon.

The current applied to the exciting coil assumed to be only inductive is

$$i(t) = \frac{V_{effexc}}{L_{exc}\omega}\sqrt{2}sin(\omega t),$$ (14)

where V_{effexc} and L_{exc} correspond to the rms voltage and the inductance of the excitation coil.

As the B magnetic field can be neglected out of the resonating ribbon, it is expressed as

$$B = \mu \cdot n_l \cdot i$$ (15)

assuming an infinitely long solenoid coil where n_l: number of loops per unit length

From Eqs. (13)–(15), one gets than $B(z) = 2\sqrt{2} \cdot \frac{n}{l(b-a)} \frac{V_{effexc}}{L_{exc}\omega}\sqrt{2}sin(\omega t)\cdot\mu(z)$

The output voltage is calculated as: $v(t) = \frac{d\Phi}{dt} = \frac{d\left(\int_{a\frac{l}{2}}^{b\frac{l}{2}} n_l\cdot dz\cdot B(z)S\right)}{dt}$

The frequency response defined as $T = \frac{V_M}{V_{effexc}}$ where V_M corresponds to rms value of $V(t)$ is then:

$$T = T_0\left(1 + 2\frac{k_{33}^2}{1-k_{33}^2}\cdot\frac{E_{r0}+jE_{i0}}{l(b-a)}\cdot\left(\frac{e^{(-k_i+jk_r)a\frac{l}{2}}+e^{(k_i-jk_r)b\frac{l}{2}}-e^{(-k_i+jk_r)b\frac{l}{2}}-e^{(k_i-jk_r)a\frac{l}{2}}}{k_i-jk_r}\right)\right)$$

$$(With)\, T_0 = \frac{S}{L_{exc}}\cdot\frac{2n_b^2}{l(b-a)}\cdot(1-k_{33}^2)\mu^\sigma$$

The frequency response T is function of a, b, L, n_b, L_{exc}, S, μ^σ, k_{33}, η, l, Y, ρ, and f. While considering T function of T_0, which then becomes a parameter, T is function of T_0, a, b, L, k_{33}, ρ, l, Y, η, and f.

It is important to emphasize that the gain depends on not only the material parameters (L, k_{33}, η, Y), but also on the size and position of the pick-up coil (a, b, and l).

A typical response is plotted in **Figure 9b**. The resonant frequencies, noted f_{rk} and f_0 or f_r for the fundamental one can be estimated from Eq. (4). The anti-resonant frequencies, f_{ak}, are not observable when studying strain response (**Figure 9a**). One observes in **Figure 9b** reversal of some anti-resonant harmonic frequencies when they are smaller than the resonant frequency: details are reported in [12].

5. Applications of magnetostrictive resonator's characterization

This model allows interestingly to estimate the values of k_{33}, η, Y, T_0, from a frequency response, providing that a, b, L, l, and ρ are known [12]. The strategy consists first in saving couples of data (f, T) from a classic analyzer and then to fit them using a least squares method to determine the set (k_{33}, η, Y, T_0). In addition, from Eq. (1), $k_{33} = d_{33}\sqrt{\frac{Y^H}{\mu_{33}^\sigma}}$, it becomes possible to estimate the value of d and then by integration that of strain λ. **Figure 10** displays the different data characteristic of Vitrovac sample. It is important to emphasize that the present contactless and cheap method is well suitable to characterize soft magnetic resonators.

6. Influence quantities

The frequency response of a resonator is strongly dependent on its geometry such length L, its physical properties (μ^σ, Y, ρ), and the operating conditions. But, some particular quantities may influence the sensing response of the magnetostrictive resonators.

6.1. Effects of field and temperature

6.1.1. Effect of field

The magnetostrictive effects depend obviously on magnetic field which is an unavoidable influence quantity, but easily quantified. The thicker line in **Figure 11** describes the variation of resonant frequency, at 20°C, versus the applied field. From Eq. (4), resonant frequency
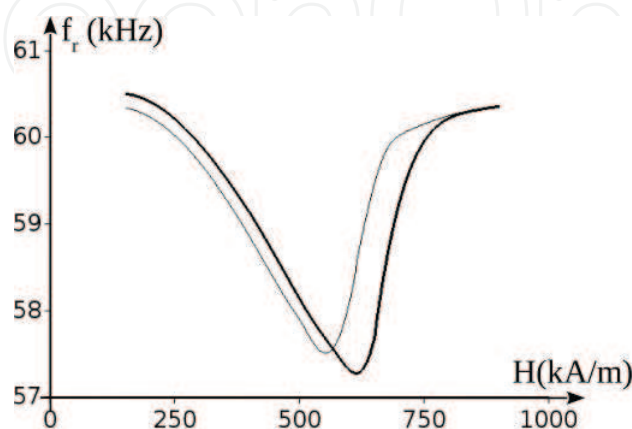

Figure 11. Evolution of magnetostriction curves for 20°C and 100°C (thick and thin line, respectively).

appears as a function of $Y^{1/2}$ assuming the density constant, also labeled as ΔY effect [13]. The variations of d or k_{33} versus the field are sources of perturbation and can be considered as influence quantities which are intrinsic to the material: consequently, one does control that d remains constant in a wide range, i.e., Ni is a better choice than amorphous ribbon.

6.1.2. Effect of temperature

As magnetization decreases with temperature, magnetostriction does the same. **Figure 11** compares frequency response versus magnetic field for two temperatures for our ribbon (thicker line corresponds to 20°C and the thinner one to 100°C) [14]. One concludes that increasing the temperature increases the minimum of resonant frequency, but decreases k_{33}. The temperature proves as an important influence quantity with change of resonant frequency up to 15%. This effect can be reduced by tuning the DC field lower than the anisotropy field while that of the thermal expansion can be neglected.

6.2. Effect of a mass stuck on the surfaces

Any mass coated on the resonator tends to absorb vibrations: the effect of inertial mass Δm coating the resonator has to be studied, assumed to be uniformly applied. In Eq. (2), the mass of the system, a slice of thickness dx, changes from $dm = \rho \cdot e \cdot d \cdot dx$ to $\rho \cdot e \cdot d \cdot dx + \Delta m \frac{dx}{L}$. This change acts equivalent to that of density from ρ to $\rho\left(1 + \frac{\Delta m}{L\rho eh}\right)$. Then the resonant frequency becomes:

$$f_0 = \frac{1}{2L}\sqrt{\frac{Y}{\rho\left(1 + \frac{\Delta m}{L\rho eh}\right)}} \tag{16}$$

It is expected only a decrease of f_0. Indeed, one observes a decrease of the maximum due to the losses generated by the friction between the resonator and the coating mass.

6.3. Effects of operating conditions

Any cause of frictions originates from an influence quantity, among them the viscosity and the density of the fluid wrapping the resonator [10]. An increase of viscosity increases the losses of the resonator and then affects damping ratio η. Such an effect can be quantified by comparing the frequency responses corresponding to two different values of damping: one expects a decreasing of the maximum concomitant to the decrease of the resonant frequency which significantly differs when the damping ratio increases (see Eq. (4)). Consequently, the attachment of the resonator disturbs strongly the frequency response.

7. Magnetostrictive sensors

7.1. Freezing-rain sensor, an emblematic example

Freezing-rain sensors which are the emblematic examples of magnetostrictive resonators, particularly because of the non-contact measurement, are used to detect the icing conditions

from the mass deposition of ice layer stuck on their surface as well as its growth [15]. The aerospace manufacturer Goodrich™ proclaims that "its sensor detects the presence of icing conditions so that appropriate actions can be taken to prevent damage to power and communication lines, to warn of road hazards, or to keep ice off wind turbine blades or a plane's wings." It is also announced that "surfaces are automatically defrosts itself when ice accumulation reaches 0.5 mm." Technical available information (including natural resonant frequency: 40 kHz, frequency decreases to 130 Hz, strut height of 2.54 cm, and strut diameter: 3.10 cm, the material is a nickel alloy rod) allows us to make some calculations. But boundaries' conditions differ from our model: free at both ends, here fixed-free than the frequency is $f_0 = \frac{1}{4L} \cdot \sqrt{\frac{Y}{\rho}}$, in our case the displacement in the middle is zero, it appears the ribbon fixed in the middle. Taking Young's modulus and density of nickel, respectively 200 GPa and 8908 kg.m^{-3}, from a length of 2.54 cm gives a frequency of 47 kHz.

The frequency, for a cylindrical resonator, with a thickness of ice e_{ice} is given by

$$f_0 = \frac{1}{4L} \sqrt{\frac{Y}{\rho \left(1 + \frac{\rho_{ice}\left((d+e_{ice})^2 - d^2 \right)}{\rho \, d^2} \right)}} \tag{17}$$

Thus, the values of the resonant frequency and its shift are estimated at 47 kHz and 85 Hz using Ni resonator, which are rather consistent with those given the manufacturer (40 kHz and 130 Hz) obtained with Ni based alloy resonator. Finally, we do emphasize that the sensitivity of the sensor is essentially due to the strut diameter (see Eq. (17)).

7.2. Chemical sensor

Magneto-elastic sensors can be used to detect chemicals such as carbon dioxide [16] or ammonia [17], biological cells [18], or to measure pH [19]. The principle is to detect the mass of chemical or biomass stuck on the surfaces. Using amorphous ribbon, the sensibility is excellent. The difficulty is to functionalize the surface in such a way that the product to be detected sticks the surface and no other contaminating elements. Ruan et al. describe the functionalization process to design a sensor for measuring ricin in solution [19]. The sample is first cut using a computer controlled laser cutter. Then it is coated with a 10 nm Cr layer and a 140 nm protective Au layer, with appropriate annealing treatment before functionalization. Magnetostrictive sensors act as excellent platforms to detect very low mass while the wireless and passive nature of these devices allows remote measurements.

7.3. Electronic article surveillance

Magnetostrictive resonators are involved in anti-theft tags which are fixed to merchandise. Tags consist of two mechanically independent free strips, one of a magnetostrictive amorphous ferromagnetic ribbon, and the second one of a magnetically semi-hard film acting as biasing magnet and switch to activate and deactivate the sensor. The good magneto-elastic coupling of the first strip originates the conversion of magnetic energy into mechanical vibrations. Detection gantries emit bursts at frequency close to that of the resonator (58 kHz) inducing thus longitudinal vibrations, which continue even after the burst is over. It results some change in

magnetization of the amorphous strip and induces thus an AC voltage to activate the detection gantry's antenna. These tags which are thicker than electromagnetic ones are cheaper and have better detection rates, but vibration and therefore detection can be deleted, when the sensor is submitted to a mechanical pressure (that of the robber!).

7.4. Magnetic sensor, thermometer, and others

The resonant frequency depends on both magnetic field and temperature which can be also measured by a resonator. Garcia-Ambas et al. [14] have investigated the possibility of temperature measurements from the temperature dependence of the magneto-elastic resonance frequency: it occurs when the magnetic biasing field applied to the resonator is close to its anisotropy field. But the sensitivity of the measurement is dependent on the temperature dependence of the magneto-elastic, which is self-correlated to that of the anisotropy constants; these low prize magnetostrictive sensors have the great advantage to make remote measurements. In addition, they can be also involved for differential and multiple measurements. Literature reports several possible applications such as stress [20] and strain [21] measurements or environmental parameters such as viscosity [22].

8. Conclusion

The aim of this chapter deals with an overview of magnetostrictive resonators, their own principles and their respective performances including sensing application domains and limitations. The development of some analytical model allows the characteristics of magnetostrictive to be estimated and the main influential quantities to be defined: thus, it does facilitate the design of new ribbon-shaped resonator suitable for specific applications.

Author details

Yannick Le Bras* and Jean-Marc Greneche

*Address all correspondence to: yannick.le_bras@univ-lemans.fr

Institut des Molécules et Matériaux du Mans, IMMM - UMR CNRS 6283, Université du Maine, Le Mans, France

References

[1] Hartemann P. Effets et matériaux magnétostrictifs. Techniques de L'ingénieur. 1999;**E1880**: 1-13

[2] du Trémolet de Lacheisserie E. Magnétisme, Tome 1, Fondements. Édition Diffusion Presse Sciences; 1999. 496 p. ISBN: 2706108312

[3] Hristoforou E, Ktena A. Magnetostriction and magnetostrictive materials for sensing applications. Journal of Magnetism and Magnetic Materials. 2007;**316**:372-378. DOI: 1016/j.jmmm.2007.03.025

[4] du Trémolet de Lacheisserie E. Magnetostriction: Theory and Applications of Magnetoelasticity. Amsterdam: CRC Press; 1993. 408 p. ISBN: 0849369347, 9780849369346

[5] Jiles DC. Recent advances and future directions in magnetic materials. Acta Materialia. 2003;**51**:5907-5939. DOI: 10.1016/j.actamat.2003.08.011

[6] du Trémolet de Lacheisserie E.: Magnétisme, Tome 2, Matériaux et Applications. Édition Diffusion Presse Sciences, 1999. 510 p. ISBN: 2706108320

[7] TdVib. Terfenol-D [Internet]. 2016. Available from: http://tdvib.com/terfenol-d/# [Accessed: June 06, 2017]

[8] Lupu N, Chiriac H, Ababei G, Grigoras M, Valeanu M, Buruiana T, Harabagiu V, Mihalca I. New 3-D bulk shaped polycrystalline and nanocomposite magnetostrictive materials. In: European School on Magnetism/Workshop on Advanced Magnetic Materials; 9–18 September 2007; Cluj-Napoca, Romania; 2007

[9] Hathaway KB, Spano ML. Measurement of high magnetomechanical coupling factors by resonance techniques. Journal of Applied Physics. 1984;**84**:1765-1767. DOI: 10.1063/1.333470

[10] Grimes CA, Mungle C, Zeng K, Jain M, Dreschel W, Paulose M, Ong K. Wireless magnetoelastic resonance sensors: A critical review. Sensors. 2002;**2**(7):294-313. DOI: 10.3390/s20700294

[11] Le Bras Y, Mazaleyrat F, Greneche JM. Analytical model of the magnetostrictive ribbon shape resonator frequency response. Sensor Letters. 2011;**9**:1801-1806. DOI: 10.1166/sl.2011.1714

[12] Le Bras Y, Lasheras A, Gutierrez J, Mazaleyrat F, Greneche JM. A new magneto-elastic resonance based technique to determine magneto-mechanical parameters of amorphous ferromagnetic ribbons. The Review of Scientific Instruments. 2013;**84**(4):043904. DOI: 10.1063/1.4799177

[13] Gutiérrez J, García-Arribas A, Garitaonaindia J, Barandiarán JM, Squire PT. ΔE effect and anisotropy distribution in metallic glasses with oblique easy axis induced by field annealing. Journal of Magnetism and Magnetic Materials. 1996;**157–158**:543-544. DOI: 10.1016/0304-8853(95)01119-6

[14] Garcia-Ambas A, De Cos D, Gutierrez J, Barandiaran JM. Selectable temperature sensitivity of the magnetoelastic resonance. Sensors and Actuators A. 2003;**106**:111-116. DOI: 10.1016/S0924-4247(03)00146-8

[15] Campbell Scientific. 0871LH1 Freezing-Rain Sensor [Internet]. 2017. Available from: https://www.campbellsci.com/0871lh1 [Accessed: June 06, 2017]

[16] Cai QY, Cammers-Goodwin A, Grimes CA. A wireless remote query magneto-elastic CO_2 sensor. Journal of Environmental Monitoring. 2000;**2**:556-560. DOI: 10.1039/b004929h

[17] Cai QY, Mahaveer KJ, Grimes CA. A wireless, remote query ammonia sensor. Sensors and Actuators. 2001;**B77**:614-619. DOI: 10.1016/S0925-4005(01)00766-3

[18] Ong K, Wang J, Singh R, Bachas L, Grimes CA. Monitoring of bacteria growth using a wireless, remote query resonant-circuit sensor: Application to environmental sensing. Biosensors & Bioelectronics. 2001;**16**:305-312. DOI: 10.1016/S0956-5663(01)00131-2

[19] Ruan C, Varghese OK, Grimes CA. A magneto-elastic ricin immunosensor. Sensor Letters. 2004;**2**:138-144. DOI: 10.1166/sl.2004.041

[20] Barandiaran JM, Gutierrez J. Magneto-elastic sensors based on soft amorphous magnetic alloys. Sensors and Actuators A. 1997;**59**:38-42. DOI: 10.1016/S0924-4247(97)80145-8

[21] Kouzoudis D, Mouzakis DE. A 2826MB Metglas ribbon as a strain sensor for remote and dynamic mechanical measurements. Sensors and Actuators A. 2006;**127**:355-359. DOI: 10.1016/j.sna.2005.12.014

[22] Grimes CA, Kouzoudis D. Remote query measurement of pressure, fluid-flow velocity, and humidity using magneto-elastic thick-film sensors. Sensors and Actuators. 2000;**84**:205-212. DOI: 10.1016/S0924-4247(00)00306-X